Military Technical College
Kobry El-Kobba,
Cairo, Egypt

11-th International Conference
on Aerospace Sciences &
Aviation Technology

ATOMIZER EFFECT ON COMBUSTION CHAMBER FLOW CHARACTERISTICS

Ola Rashed[1], Badiea Hafez[2] and Antal Penninger[3]

ABSTRACT

Liquid fuel combustion systems atomize the fuel prior to combustion in order to enhance combustion performance. The combustion depends strongly on the atomization process. The objective of this work is to determine the suitable atomizer for the different combustion systems. A mathematical model describing the flow emerging from the atomizer throughout the combustion chamber is developed. Comparisons are drawn between Airblast and Simplex atomizers, so that the atomizer type effect on the flow characteristics is determined.
By producing smaller Sauter Mean Diameters (SMD), Airblast atomizer have droplet evaporating time is consequently less; proven to be more efficient and therefore airblast atomizers are more in use in industry. While Simplex atomizers are in demand when a wide spray cone angle is required. Also some initial conditions impose the simplex choice because of combustion instabilities occurring when using airblast atomizers with these input in the combustion chamber conditions.

KEY WORDS
Atomizer, Combustion Flow Characteristics, Combustion modeling

---

[1] Professor, Cairo University, Faculty of Engineering, Aerospace Department
[2] Assistant Professor, Cairo University, Faculty of Engineering, Aerospace Department
[3] Professor, Head of the Heat Engines Department, Budapest Technical University

NOMENCLATURE

A	Droplet surface area
B_M	Mass transfer number
B_T	Heat transfer number
C_D	Drag coefficient
C_l	Specific heat of liquid
C_P	Specific heat at constant pressure
C_v	Specific heat at constant pressure
d_k	Instantaneous diameter of k^{th} droplet
d_o	Initial droplet diameter
D_c	Diffusion coefficient
D_k	Drag function
h	Enthalpy
k	Thermal conductivity
L	Latent heat of vaporization
L_e	Lewis number
L_r	Ratio of gas-phase length scale and initial droplet radius
L_c	Gas-phase length scale
m_k	Mass of k^{th} droplet
$\dot{m}_k$	Mass evaporation rate of k^{th} droplet
Nu	Nusselt number
p	Pressure
Pr	Prandtl number
Q_g	Energy transferred from gas-phase to droplet
Q_l	Liquid heating energy
r_k	Radius of k^{th} droplet
R	Ideal gas constant
Re	Reynolds number
Re_o	Initial Reynolds number
S_e	Energy exchange term between two phases
S_m	Mass exchange term between two phases
S_M	Momentum exchange term between two phases
t	Time
t_r	Ratio of convective time scale to diffusive time scale in gas-phase
T	Temperature
T_B	Boiling temperature
T_l	Liquid drop temperature
u	Gas-phase velocity
v	Droplet velocity
x	Droplet position
Y	Mass fraction
$\delta(x)$	Dirac delta function
ΔV	Cell control volume
μ	Dynamic viscosity
ν	Kinematic viscosity
ρ	Density
τ	Non-dimensional time

Subscripts

a	air
g	gas
l	liquid
k	k^{th} droplet
v	vapor
o	initial
∞	Unperturbed conditions

INTRODUCTION

Spray atomization in gaseous atmosphere is of importance to industrial processes involving spray combustion, or spray evaporation. The liquid atomization process is short and depends mainly on nozzle configuration, jet injection velocity, liquid properties ambient conditions [1]. Once the liquid is dispersed into droplets, the interfacing area between the liquid and gas is greatly increased, with the heat and mass transfer processes being dramatically enhanced. Consequently, the atomization process affects the dynamics and thermal processes of any droplet. Thus the installation of any specific atomizer is dictated by the flow characteristics needed. The objective of this work is to provide a numerical model for facilitating the choice of the appropriate atomizer. Studies regarding atomizer performance usually focus on one kind of atomizers. Previous investigations of significance are those of Nukiyama and Tanasawa [2], Weiss and Worsham [3], Gretzinger and Marshall [4], Kim and Marshall [5], Lorenzetto and Lefebvre [6], and Jasuja [7]. All these studies concerning airblast atomization elucidated key factors and its range of study were incomplete. Except for Jasuja, who made no attempt to determine the drop size distribution in the spray, the experiments conducted in these research efforts covered only atmospheric pressure. On the other hand a fairly wide range of atomizing air velocity, fuel viscosity, air/fuel ratio, and atomizer geometry was covered. Risk and Lefebvre [8] focused on the effect of ambient pressure on mean drop size and drop size distribution. As determined by Lefebvre et al and El Kotb [9,10] drop size distribution is of utmost importance, for it determines the evaporation history. They proved that sprays with a non-uniform drop size distribution evaporates more rapidly in the initial phase than do sprays of the same mean diameter, due to the presence of a larger number of small drops.
Most previous research on atomization has naturally concentrated on the most widely used types of fuel injectors. For example the effervescent Diesel injector was the subject of Wade et al. [11], Sovani et al. [12], Sutherland et al. [13,14], and Luang et al. [15]. They experimentally tied the drop size distribution to atomizing gas-liquid ratio, injector pressure, and also to nozzle geometry. The air-assist pressure swirl atomizers has its share of studies also, performance and limitations were reported by Schmidt et al. [16].
Numerical studies tackled the problem of sprays by performing an analysis on the influence of operating conditions on drop size distribution [17,18].
The goal of this work is to provide a numerical algorithm, which enables the choice of the appropriate atomizer according to operating conditions needed. The developed computer program main contribution is the tying of the drop size distribution calculation for the injector of choice, with the combustion chamber governing equations. This flow is modeled so that the combustion chamber characteristics are coupled to the atomizer performance. The present code solves the combustion chamber flow by using a separated flow approach (SF). Numerous SF models with different assumption had been proposed to consider this complex inter-phase phenomena [19,20,21]. Integrating these different assumptions, the present computer algorithm takes the inter-phase transport phenomena, the quasi-steadiness of the droplet boundary layer, the variable coupled phase properties,

slip, gas film non-unitary Lewis number, the Stefan flow, transient liquid heating and internal droplet circulation into consideration.

PHYSICAL MODEL

The flow entering the injector of choice is modeled so that the emerging drop size distribution is obtained. The SMD is calculated and the combustion chamber flow is modeled. It is assumed that upon injection the fuel ligaments start to break forming spray droplets. This accelerating fuel spray consists of droplets of variable sizes. The droplet internal circulation is initiated and the combustion gases response to the droplet presence by surrounding each one with a mass and a thermal boundary layer. The droplets are modeled throughout the variable temperature and velocity field combustion flow. The continuity, momentum, and energy equations, in addition to the state equation govern this flow. Invoking the incompressible flow conditions the droplets are governed with similar equations. Strong coupling exists between the liquid and gas phases; thus an iterative procedure is used to solve these equations simultaneously.
The present code was run for the simplex and the airblast atomizers as test cases. Comparison with the previous experimental and numerical work proved this work to be accurate.

GOVERNING EQUATIONS

Atomizer Equations

In order to model the problem mathematically, we are faced with determining the drop size distribution, which is most difficult to predict theoretically or to determine experimentally. Referring to Nukiyama and Tanasawa [2] a relative simple mathematical function that adequately describes the distribution is used:

$$\frac{dN}{dD} = aD^{p} \exp -(bD)^{q} \qquad (1)$$

where N and D are the number of droplets and the drop diameter respectively; and a,b,p,q are constants dependent on the atomizer geometry and operating condition. Referring to Lefebvre [1] and El Kotb [10] the distribution function is completely defined at different atomizer operating conditions, and the four (a, b, p, q) parameters of the distribution function are deduced at different atomizer inlet velocities and pressures. Then the Sauter Mean Diameter SMD is calculated according to

$$\frac{\sum N_I D_I^3}{\sum N_I D_I^2} \qquad (2)$$

where I denotes the size range considered, N_I is the number of drops in the size range I, and D_I is the middle diameter of size range I.

Gas-Phase Equations

The droplets are injected in a gaseous medium, so they are considered to be sources of mass and momentum, as well as sinks of energy. The gas phase governing equations describing the model can be written in general as following

$$\frac{\partial \rho_g}{\partial t} + \nabla(\rho_g v_g) = S_m$$

$$\frac{\partial(\rho_g v_g)}{\partial t} + \nabla(\rho_g v_g v_g) = \nabla(\rho_g \upsilon_g \nabla v_g) - \nabla(p) + S_M$$

$$\frac{\partial(\rho_g h_g)}{\partial t} + \nabla(\rho_g v_g h_g) = \nabla(k_g \nabla T_g) + S_e \qquad (3,4,5,6)$$

$$\frac{\partial(\rho_g Y_v)}{\partial t} + \nabla(v_g \rho_g Y_v) = \nabla(\rho_g D_c \nabla Y_v) + S_m$$

exchange terms, respectively, and are defined as

where p, ρ, v, T, and t are the pressure, density, velocity, temperature and time respectively. The vapor-mass fraction Y_v is defined as

$$Y_v = \frac{\rho_v}{\rho_g}$$

The quantities S_m, S_M, and S_e represent the mass, momentum, and energy

$$S_m = \frac{t_r}{L_r} \sum n_k \frac{\dot{m}_k}{\Delta V}$$

$$S_M = -\sum_k D_k (v_{g,e} - v_k) \delta(x - x_k) / \Delta V \qquad (7,8,9)$$

$$S_e = -\sum_k \delta(x - x_k) \left[\dot{m}_k L + C_l m_k \frac{dT_k}{dt} + \dot{m}_k C_v \left(T_{g,e} - T_k \right) \right] / \Delta V$$

where
ρ_r, L_r, t_r are the gas density ratio, the gas-phase length scale, and the convective to diffusive time scale ratio respectively, and are defined as

$$\rho_r = \frac{\rho_{go}}{\rho_l}$$

$$L_r = \frac{\delta_m}{r_{ko}}$$

$$t_r = \frac{t_c \delta_m}{D_c}$$

t_c is the time consumed in forming δ_m, the mass boundary layer, which is obtained from the heat transfer solution.
The ideal-gas equation of state is also adopted.

$$P = \rho_g [R_a + Y_v (R_v - R_a)] T_g \qquad (10)$$

The gas-phase governing equations are solved to obtain the gas flow characteristics, by using a 2nd order Runge-Kutta technique for the equation of mass and energy and a numerical explicit finite difference scheme for the species and momentum equations. The liquid-phase solution is used as input to this scheme and then iteration is performed to insure the correctness of the obtained results.

Liquid - Phase Equations

Droplet Motion Equations

According to Abramzon and Sirignano [26]and to Aggarwal [27], each droplet, labeled by a subscript k is assumed to obey the following equations:

$$\frac{dx}{dt} = V_k$$

$$\frac{dV_k}{dt} = \rho_r L_r^2 t_r \left(\frac{3}{16} \frac{C_D \mu \mathrm{Re}_k (V - V_k)}{r_k^2} \right) \qquad (11,12,13)$$

$$\frac{dr_k^2}{dt} = -2 \rho_r L_r^2 t_r M_k$$

where the M_k is obtained from the heat transfer equation solution and is defined as follows

$$M_k = \left(1 + 0.3\,\mathrm{Re}_k^{\frac{1}{2}}\right)\ln(1 + B_M)$$

$$B_M = \frac{Y_{fs} - Y_{f\infty}}{1 - Y_{fs}}$$

B_M is the mass transfer number (referred to as Spalding number).

the particle Reynolds number Re_k and the drag coefficient C_D are defined as follows

$$C_D = \frac{24}{\mathrm{Re}_k}\left(1 + \frac{\mathrm{Re}_k^{\frac{2}{3}}}{6}\right)$$

$$\mathrm{Re}_k = \frac{2 r_k \rho}{t_r L_r \mu}\left|V - V_k\right|$$

According to Aggarwal [27], Re_k is covering all the range above 100. In order to obtain the velocity of the droplets, the distance traveled, the droplet radii, these governing equations are solved using a 2nd order Runge- Kutta Scheme. The obtained results are then used as input for the gas phase problem, and the iterative procedure is performed until convergence is reached.

Droplet Mass & Heat Transfer equations

As described by Feath [22], the droplet heat-up and evaporation calculations use the following correlations to obtain the mass & heat transfer rates

$$\frac{\dot{m}_k d}{\rho D_f} = 2N_s \ln(1 + B_M) \qquad (14)$$

$$\frac{hd}{k} = 2N_p \frac{\ln(1 + B_M)^{Le-1}}{\left((1 + B_M)^{Le-1} - 1\right)} \qquad (15)$$

where h, d, D_f, k, and $\dot{m}_k$ are the heat transfer coefficient, the droplet diameter, the fuel-mass diffusivity, thermal conductivity and mass evaporation rate per unit area. For effective computational time and accuracy, an " effective value of

the liquid thermal conductivity k " is used to calculate and to account for the droplet internal circulation, which influences the heat transfer within the droplet. The N_s and N_p are defined as:

$$N_s = 1 + \frac{0.276\,\mathrm{Re}^{\frac{1}{2}}\,\mathrm{Pr}^{\frac{1}{3}}}{\left(1 + \frac{1.232}{\mathrm{Re}(\mathrm{Pr}^{\frac{4}{3}})}\right)^{\frac{1}{2}}}$$

and

$$N_p = 1 + \frac{0.276\,\mathrm{Re}^{\frac{1}{2}}\,Sc^{\frac{1}{3}}}{\left(1 + \frac{1.232}{\mathrm{Re}(Sc^{\frac{4}{3}})}\right)^{\frac{1}{2}}}$$

Sc and Le are the Schmidt and Lewis numbers.
In order to evaluate the mass and the thermal boundary layer thickness the effect of the Stefan flow on the heat and mass transfer had to be accounted for by a correction factor F on both thicknesses.

$$F_M = (1 + B_M)^{0.7}\,\frac{\ln B_M}{B_M}$$

$$F_T = (1 + B_T)^{0.7}\,\frac{\ln B_T}{B_T}$$

where

$$B_T = \frac{T_\infty - T_k}{h}$$

Then the thermal and boundary film thickness δ_T and δ_m are evaluated by using the following relations:

$$F_M = \frac{\delta_M}{\delta_{Mo}}$$

$$F_T = \frac{\delta_T}{\delta_{To}}$$

where

$$\delta_{Mo} = \frac{2r_S}{(Nu_o - 2)}$$

$$\delta_{To} = \frac{2r_S}{(sh_o - 2)}$$

the Nusselt and Sherwood numbers at the initial condition (o) are obtained as follows

$$Nu_o = 2 + 0.552\,\mathrm{Re}^{\frac{1}{2}}\,\mathrm{Pr}^{\frac{1}{3}}$$

$$sh_o = 2 + 0.552\,\mathrm{Re}^{\frac{1}{2}}\,Sc^{\frac{1}{3}}$$

Droplet internal Temperature Equations

The temperature distribution within the droplet is obtained by solving the energy equation subject to the convective boundary conditions at the droplet surface by a Crank- Niclson scheme.

$$\frac{\partial T_1}{\partial t_b} = \frac{\partial^2 T_1}{\partial \tilde{r}^2} + \left(\frac{2}{\tilde{r}} - \tilde{r} M_k K\right)\frac{\partial T_1}{\partial \tilde{r}} \qquad (16)$$

with the following initial and boundary condition

$$T_1(\tilde{r},0) = 0$$

$$\frac{\partial T_1}{\partial \tilde{r}} = \frac{C_k M_k}{(T_B - T_o)}(h - L)$$

Where $\tilde{r}$, L, and C_k are the radial distance within the droplet, the latent heat of evaporation, and the specific heat respectively. B and h are obtained from the heat transfer equations.

The choice of the increments used in the Partial Differential Equations is of crucial importance to the solution; smaller increments tend to give accurate results. Staggered meshes are applied in the physical domain to facilitate the discretization schemes. The increments yielding good results were Δ x = 0.001mm, and Δ t ranging between 0.001 ms and 0.0001 ms. The program showed instabilities when the increments where further reduced to Δ x= 0.00001 mm and Δt= 0.000001 ms.

It is worth mentioning that:

The average physical properties (T, Cp_g, μ_g, Kg, T, D, C p_f, ρ) are calculated by the following 1/3 rule [23]

$$\Phi = \Phi s + 1/3\,(\Phi g - \Phi s)$$

SOLUTION PROCEDURE

A multi-step iterative procedure is used at each time interval for solving the governing equations. The computational domain starts from x=0.5 D_P to the diminishing of the droplet. The initial and boundary conditions are taken interchangeably form the gas and liquid phases, the calculations proceeded as follows:

1. The Sauter Mean Diameter is calculated for each set of input conditions.
2. Contributions to the dependent variables in the flow governing equations are calculated.
3. The liquid-phase equations for conservation of mass and momentum are first solved by means of a second order Runge-Kutta scheme.
4. The pressure and its contribution to the dependent variables is solved taking into account the effect of surface tension forces on interface momentum transfer.
5. With the droplet velocity, distance traveled, and droplet radii obtained in step2, the droplet mass and heat transfer, droplet surface and core temperatures, and the viscous and thermal boundary layers were calculated by solving the droplet energy, heat and mass transfer equations using a Crank-Niklson scheme.
6. The solutions of steps 2 and 5 are used in an explicit finite difference scheme to solve the gas-phase continuity, momentum, energy and species equations to obtain the gas density, pressure, velocity, mass fraction, and interfacial shear stresses and drag.
7. The physical gas and liquid properties and the Hill vortex strength are updated. Iteration between steps 2 – 6 is carried out until the required convergence is achieved. When the obtained temperature difference from two consecutive calculations equals 0.001 the step convergences. Then the flow characteristics are evaluated for this time step.
8. Steps 2-7 are repeated for an advanced time with the updated flow conditions.

RESULTS AND CONCLUSIONS

Airblast atomizers produce droplets with smaller diameters than simplex atomizers. The fuel must be pumped at a relatively high pressure in order to obtain fine droplets from the simplex atomizer. Therefore for the same initial conditions, droplets from airblast atomizers evaporate in less time. Consequently when using airblast atomizers, the combustion chamber becomes more compact. However the flow characteristics vary with the atomizer type used and the following results will help in the choice of atomizer type and design of combustion chamber.

Fig.1 displays the non-dimensional radius versus time for simplex and airblast atomizers. We note that the difference in droplet diameter led to different evaporating times.

Fig.2 shows the relation between droplet velocity and time for simplex and airblast atomizers. Droplets from airblast atomizers gain velocity rapidly due to their faster droplet-gas heat exchange.
Fig.3 displays liquid Reynolds number versus time. Due to the difference in initial droplet diameters, there is a difference in the initial liquid Reynolds number.
Being larger in diameter, the droplet from simplex atomizers takes longer time in order to exchange heat, therefor its velocity and evaporation rate is less. This is reflected in the liquid Reynolds number behavior throughout the droplet lifetime.
The gas Reynolds number is calculated using the velocity,density and kinematic viscosity obtained in each time step. Fig.4 shows the relation between gas Reynolds number versus time. The difference in the initial value of gas film Reynolds number for both atomizers is due to the difference in the initial droplet diameter.
Fig.5 shows that Lewis number versus time. The Lewis number is related to the rate of energy and mass exchange. Droplets from simplex atomizers take more time than those from airblast atomizers to evaporate; thus the Lewis number decreases more rapidly for airblast atomizer than for the simplex one.
Fig.6 displays the droplet surface temperature versus time.
The droplet surface temperature, for droplets with smaller diameters increases more rapidly than for the larger droplets. For the same initial conditions higher combustion performance is obtained when using airblast atomizers because it sprays finer droplets.
The computer code has been validated against work done by Sirignano [24] and Chiang [25]. The same cases tackled by these scientists were calculated using the present code. The obtained results are compared with their values. Fig.7 shows the droplet diameter comparison, and Fig.8 shows the droplet surface temperature comparison. Fig.9 and Fig.10 show the simplex and the airblast atomizers used in this study. The two atomizers are chosen according to Lefebvre [1]. As seen from the figures the present work is in good agreement with data obtained by the previously mentioned researchers. However the ease of use and the accurately accounted for different inter-phase phenomena is in favor of this computer algorithm.

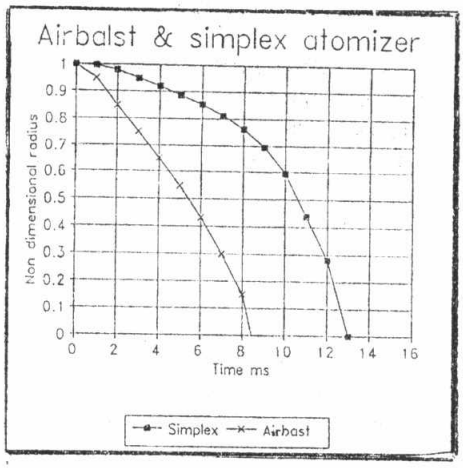

Fig.1. Non-Dimensional Radius vs. Time

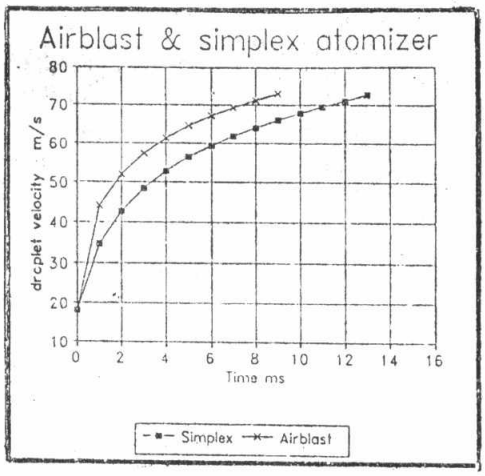

Fig.2.Droplet Velocity vs. Time

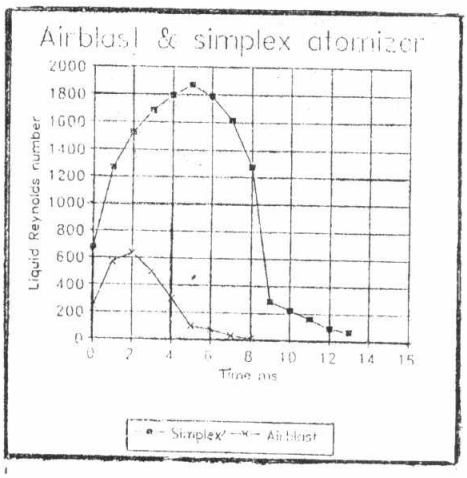

Fig.3.Liquid Reynolds No. Vs. Time

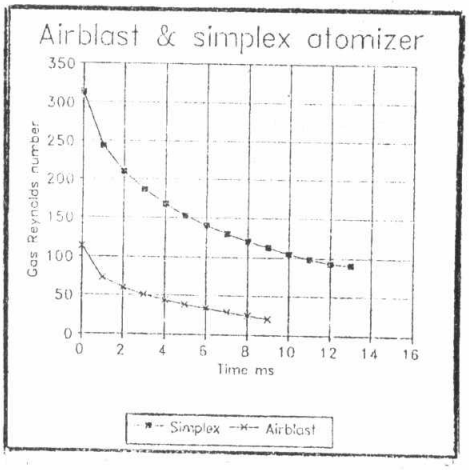

Fig.4.Gas Reynolds No Vs Time

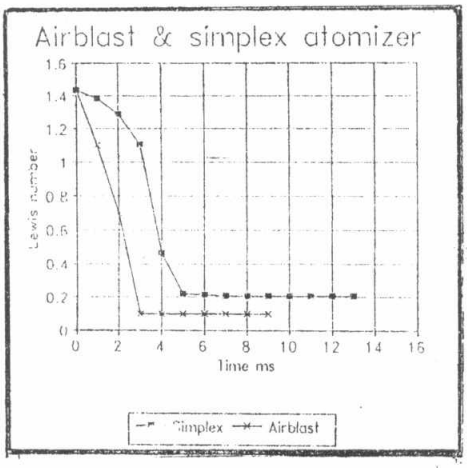

Fig.5. Lewis No. Vs. Time

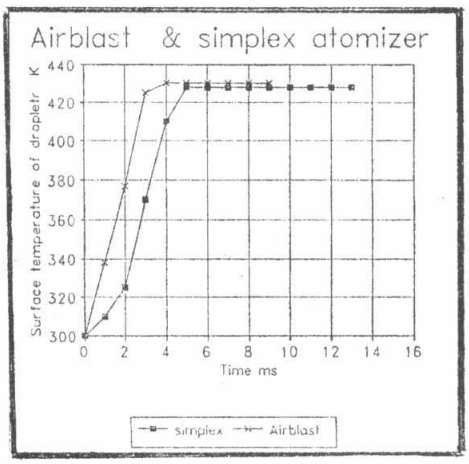

Fig.6. Droplet Surface Temperature Vs. Time

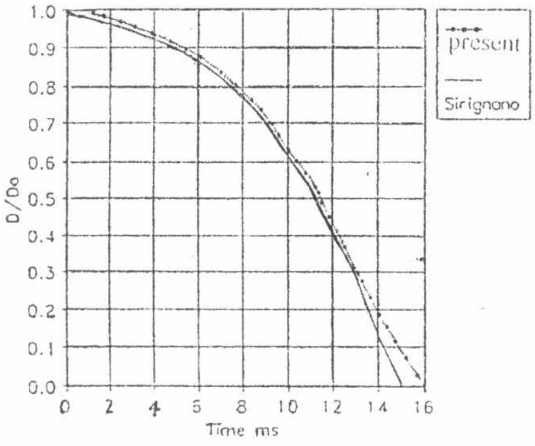

Fig.7. Droplet Diameter Comparison

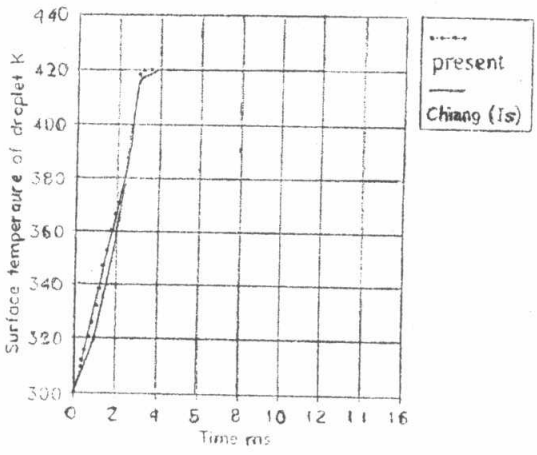

Fig.8. Drop Surface Temp Comparison

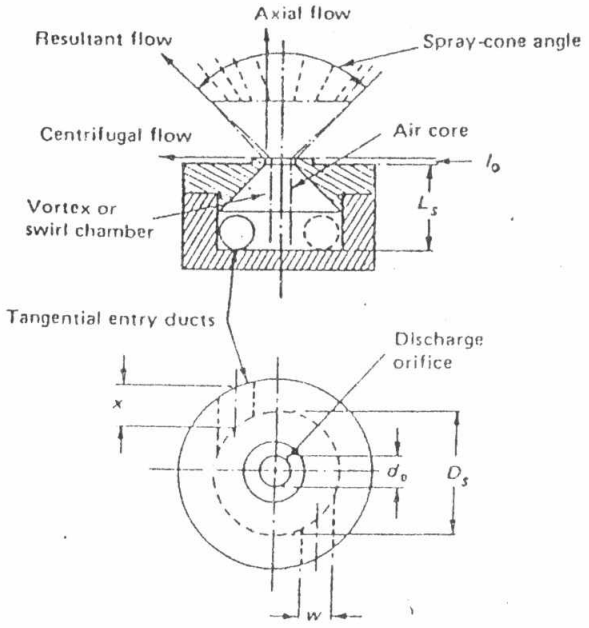

Fig.9 Simplex Atomizer

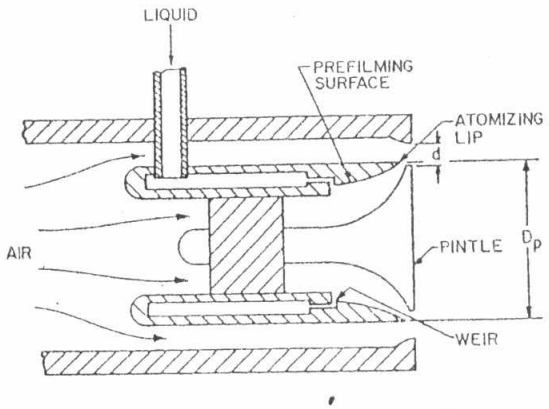

Fig.10 Airblast Atomizer

References

[1] Lefebvre, A.H. Atomization and Sprays, Hemisphere Publishing Corporation, New York, (1989)
[2] Nukiyama, S., and Tanasawa, Y, "Experiments on the Atomization of Liquids in an Air Stream" Trans. Soc. Mech. Eng. Jpn., Vol. 5, No. 18, pp. 62-67, (1939).
[3] Weiss, M.A. and Worsham, C.H. "Atomization in High Velocity Air Streams", J. Am. Rocket Soc., Vol. 29, No. 4, pp.252-259, (1959).
[4] Gretzinger, J., and Marshall, W. R. Jr., "Characteristics of Pneumatic Atomization", AIChE J., Vol. 7, No.2, pp.312-318, (1961).
[5] Kim, K. Y., and Marshall, W. R., "Drop-Size Distribution from Pneumatic Atomizers", AIChE J., Vol. 17, No.3, pp.575-584, (1971).
[6] Lorenzetto, G. E., and Lefebvre, A. H., "Measurements of Drop Size on a Plain Jet Airblast Atomizer", AIAA J., Vol. 15, No. 7, pp. 1006-1010, (1977).
[7] Jasuja, A. K., "Plain-Jet Airblast Atomization of Liquid Petrolium Fuels under High Ambient Air Pressure Conditions", ASME Paper 82-GT-32, (1982).
[8] Risk, N. K., and Lefebvre, A. H., "Spray Characteristics of Plain Jet Airblast Atomizers", Trans. ASME J. Eng. Gas Turbines Power, Vol. 106, pp.639-644, (1984).
[9] Lefebvre, A. H., Wang, X. F., and Martin, C. A., "Spray Characteristics of Aerated Liquid Pressure Atomizers", AIAA J. of Propul. Power, Vol.4, No. 4, pp. 293-298, (1988).
[10] El Kotb, M. M., "Fuel Atomization For Spray Modelling", Prog. Energy Combust. Sci., Vol. 8, pp. 61-91, (1982).
[10] Wade, R.A, Weerts, J. M., Sojka,P.E., and Gore, J.P. "Effervescent Atomization at Injection Pressure in the MPa Range" http://widget.ecn.purdue.edu/~sojka/robtwade.html , (1999).
[12] Sovani, S.D., Crofts, J.D., Sojka, P.E., Gore, J. P., and Eckerle, W.A. "Spray Performance of a Prototype Effervescent Diesel Injector", http://widget.ecn.purdue.edu/~sojka/proto.html , (1999).
[13] Sutherland, J.J., Sojka, P.E., and Plesniak, M.W. "Ligament-Controlled Effervescent Atomization", Atomization and Sprays, Vol. 7, No. 4, pp.383-406, (1997).
[14] Sutherland, J.J., Sojka, P.E., and Plesniak, M.W. "Entrainment by Ligament-Controlled Effervescent Atomizer-Produced Sprays", Int. J. Multiphase Flow, Vol. 23, No. 5, pp. 865-884, (1997).
[15] Luong, J.T.K., and Sojka, P.E., "Unsteadiness in Effervescent Sprays", Atomization and Sprays, Vol. 9, No. 1, pp. 87-109, (1997).
[16] Schmidt, U.T., and Sojka, P.E. "Air-Assist Pressure-Swirl Atomization", Atomization and Sprays, Vol. 9, No. 2, pp. 173-192, (1999).
[17] Sovani, S.D. Sojka, P.E., and Sivathanu, Y.R. "Prediction of Drop Size Distributions from First Principles: The Influence of Fluctuations in Relative Velocity and Liquid Physical Properties", Atomization and Sprays, Vol. 9, No. 2, pp. 133-152, (1999).
[18] Panchagnula, M.V., Sojka, P.E., and Santangelo, P.J., "On the Three-Dimensional Instability of a Swirling, Annular Inviscid Liquid Sheet Subject to

Unequal Gas Velocity", Physics of Fluids, Vol. 8, No. 12, pp.3300-3312, (1996).
[19] Shuen, J. S. "Prediction of the Structure of Fuel Sprays in Cylindrical Combustion Chambers," J. of Propulsion and Power, Vol. 3, p.105, (1987).
[20] Raju, M.S. and Sirignano, W.A., "Multi-component Spray Computations in a modified Center-body Combustor," J. of Propulsion and Power, Vol. 6, p. 97, (1990).
[21] Solomon, A.S.P., Shuen, J.S, Zhang, Q.F., and Faeth, G. M., "Measurement and Predictions of the Structure of Evaporating Sprays," J. of Heat Transfer, Vol. 107, p. 679, (1985).
[22] Faeth, G. M. "Evaporation and Combustion of Sprays," Prog. In Energy and Combustion Science, Vol.9, p. 1, (1983).
[23] Sparrow, E.M., and Gregg, J.L., "The Variable Fluid Property Problem in Free Convection, " in Trans. Am. Soc. Mech. Engrs , Vol. 80, 879-886, (1958).
[24] W. A. Sirignano, "Fuel Vaporization and Spray Combustion Theory," Prog. in Energy and Comb. Sci., Vol. 9, p. 291, (1983).
[25] Chiang, C.H., Raju, M.S., and Sirignano, W.A, " Numerical Analysis of Convecting, Vaporization Fuel Droplet with Variable Properties," International Journal of Heat and mass Transfer, Vol. 35,No. 5, p. 1307-1324, (1992).
[26] B.ABRAMZON and W.A.SIRIGNANO "Droplet vaporization model for spray combustion Calculations" Int. J. Heat Mass Transfer Vol32 No9, PP.1605-1618-1989
[27] SURESHK. AGGARWAL " Modeling of a dilute Vaporizing multi-component fuel spray" Int. J. Heat Mass Transfer Vol30, No (, PP. 1949-1961, 1987